RSC Advances

PAPER

View Article Online
View Journal | View Issue

Cite this: *RSC Adv.*, 2017, **7**, 25089

Determination of the crystal structure and photoluminescence properties of $NaEu_{1-x}Gd_x(MoO_4)_2$ phosphor synthesized by a water-assisted low-temperature synthesis technique†

Takuya Hasegawa, ‡[a] Sun Woog Kim,§*[a] Yusuke Abe,[a] Masaru Muto,[a] Mizuki Watanabe,[a] Tatsuro Kaneko,[a] Kazuyoshi Uematsu,[a] Tadashi Ishigaki,[a] Kenji Toda,*[a] Mineo Sato,[b] Junko Koide,[c] Masako Toda[c] and Yoshiaki Kudo[c]

Received 14th February 2017
Accepted 19th April 2017

DOI: 10.1039/c7ra01832k

rsc.li/rsc-advances

A single-phase red-emitting $NaEu(MoO_4)_2$ phosphor with nanosized particles was synthesized using a water-assisted solid state reaction (WASSR) method, a new low-temperature synthesis method developed by our group. $NaEu(MoO_4)_2$ exhibits a monoclinic structure with a space group $C2/c$ (no. 15), which is composed of a Na/EuO_8 dodecahedron with the site occupancy of $Na/Eu = 1:1$ and an MoO_4 tetrahedron. To enhance the emission intensity of the $NaEu(MoO_4)_2$ phosphor, Gd^{3+} was doped into the Eu^{3+} sites and $NaEu_{1-x}Gd_x(MoO_4)_2$ ($0 < x \leq 0.50$) samples were synthesized using the WASSR method. The emission intensity of the phosphors was successfully enhanced by increasing the Gd^{3+} content in the samples with $0 \leq x \leq 0.30$, but was reduced with $x > 0.30$. This indicates that the optimum composition of the phosphor for achieving a high emission intensity that is ~3.8 times higher than that of the $NaEu(MoO_4)_2$ ($x = 0$) phosphor is $NaEu_{0.70}Gd_{0.30}(MoO_4)_2$. These phosphors exhibit a granular particle morphology with the particle size of the phosphor being ~200 nm.

Introduction

Ceramic optical materials with nanosized particles have been widely used for new technologies, such as lighting systems, biosensing and energy devices.[1–4] In particular, phosphors dispersed in a glass or film have attracted much attention as a light convertor in white-light emitting diodes (white-LEDs) and white-laser diodes (white-LDs) and as a spectral convertor in solar-cells because of its higher dispersibility as compared with the bulk materials.[1,4–6]

Functional ceramic powder materials including phosphor materials are mostly synthesized using the solid-state reaction (SSR) method, as it is very simple and can be employed for easily synthesizing ceramic materials. However, this method requires high temperatures (>1000 °C) for obtaining single phase materials because ionic diffusion in a solid markedly increases with an increase in the reaction temperature according to the Arrhenius equation:[7]

$$k = A \exp[-E_a/k_b T]$$

where k is the velocity constant, A is the frequency factor, E_a is the activation energy, k_b is the Boltzmann's constant, and T is the temperature. However, high-temperature synthesis usually results in the particle growth and particles with irregular morphology are formed in the final product.[8] Therefore, it is difficult to synthesize ceramics powders with fine-sized particles using the conventional SSR method. In contrast, liquid phase reaction (LPR) methods, which usually employ aqueous solutions or organic solvents, have been widely investigated for obtaining functional ceramics powder materials with fine-sized particles.[9,10] Nevertheless, most of the LPR methods require special procedures, such as pH control, filtration and other processes.[9] Therefore, the cost of the ceramic powder materials synthesized by the LPR methods is higher than that obtained by the conventional SSR method. Therefore, the development of a new synthesis method without employing special processes is

[a]*Graduate School of Science and Technology, Niigata University, 8050 Ikarashi 2-nocho, Niigata, 950-2181, Japan. E-mail: ktoda@eng.niigata-u.ac.jp*

[b]*Department of Chemistry and Chemical Engineering, Niigata University, 8050 Ikarashi 2-nocho, Niigata 950-2181, Japan*

[c]*N-Luminescence Corporation, 8867-3 Ikarashi 2-nocho, Niigata 950-2101, Japan*

† Electronic supplementary information (ESI) available. See DOI: 10.1039/c7ra01832k

‡ Current address: Department of Marine Resource Science, Faculty of Agriculture and Marine Science, Kochi University, 200 Otsu, Monobe, Nankoku City, Kochi 783-8502, Japan.

§ Current address: Department of Nanotechnology and Advanced Material Engineering, Sejong University, 209 Neungdong-ro, Gwangjin-gu, Seoul 05006, Republic of Korea. skim80@sejong.ac.kr

necessary to obtain small particle ceramic materials at a low cost.

In our previous study, we developed a novel synthesis method which can be used for easily synthesizing ceramics powder materials with fine-sized particles at a low temperature (<100 °C) without employing any chemical and physical after-process treatment.[11–15] Some oxide materials can be synthesized at room temperature by mixing raw materials or by storing the mixture of raw materials at low temperatures. In addition, the reaction can be drastically promoted by adding a small amount of water. We refer this novel synthesis method as the "water-assisted solid-state reaction (WASSR) method" or the "solid hydrate thermal reaction (SHR) method". Recently, we have referred this novel synthesis method as the WASSR method because the reaction mechanisms of both WASSR and SHR are the same. The added water, which covers the particle surface of the raw materials, activates a surface reaction between them, resulting in the acceleration of the solid acid–base reaction of the raw materials. Using this method, we successfully synthesized functional ceramic powder materials containing fine-sized particles at temperatures lower than 100 °C. Additionally, we investigated the reactivity of different raw materials in solvents other than water such as acids, alcohols, and organic solvents (Table S1 in ESI†). We observed that the reaction between raw materials is either too slow or does not occur in these solvents.

In this study, we synthesized the $NaEu(MoO_4)_2$ phosphor using WASSR and their photoluminescence properties were investigated in detail and compared with those of the phosphor prepared using the conventional SSR method. The scheelite-type $NaEu(MoO_4)_2$ can be considered to be an efficient phosphor material because of its excellent thermal and chemical stability.[16] In addition, it is well-known that $NaEu(MoO_4)_2$ phosphor exhibits red emission under UV excitation.[16–19,21]

Experimental section

Preparation of the $NaEu_{1-x}Gd_x(MoO_4)_2$ phosphor

Commercial grade oxides and carbonates were used as the starting materials. Na_2CO_3 (Kanto Chem. Co. Ltd., 99.8%), Eu_2O_3 (Shin-Etsu Chem. Co. Ltd., 99.99%), Gd_2O_3 (Shin-Etsu Chem. Co. Ltd., 99.99%) and MoO_3 (Kojundo Chem. Lab. Co. Ltd., 99.98%) powders were used as the starting materials for obtaining a single-phase $NaEu_{1-x}Gd_x(MoO_4)_2$ phosphor. The powders were mixed in a stoichiometric ratio using a mortar without any solvent for 1 min. Both the mixture and a glass bottle with a volume of 3 mL containing 1 mL de-ionised water were kept in a closed polystyrene container with a volume of 10 mL, as shown in Fig. 1. The closed-container was stored at 80 °C for 48 h in an automatic oven (Yamato Scientific Co., Ltd. DKN 302). To verify the effect of the WASSR method, $NaEu(MoO_4)_2$ was synthesized using the conventional SSR method for comparison. The stoichiometric mixture was calcined at 800 °C for 10 h in air.[18]

Characterization of the $NaEu_{1-x}Gd_x(MoO_4)_2$ phosphor

The crystal structure of the phosphor samples was examined using powder X-ray diffraction (XRD; D2 PHASER, Bruker Co.).

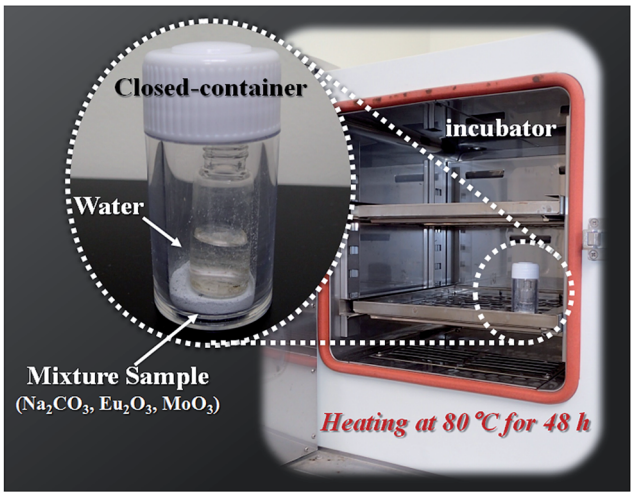

Fig. 1 Photographs of the reaction system used for the WASSR method.

For determining the crystal phases, Rietveld refinement of the obtained XRD pattern was performed using the RIETAN-FP software package.[20] Photoluminescence excitation and emission spectra of the phosphors were measured at room temperature with a spectrofluorometer (Jasco Corp. FP-6500/6600). The excitation spectra were recorded for emission at 612 nm and the emission spectra were obtained for excitation at 300 nm. The particle morphology of the phosphor samples was characterised using scanning electron microscopy (SEM; JSM-5310MVB, JEOL Ltd.).

Results and discussion

Crystal structure

In order to determine the crystal structural parameters of the $NaEu(MoO_4)_2$ phosphor synthesized by the WASSR method, we carried out the Rietveld analysis on the powder XRD data for all the space groups obtained in the early refinement stages. The monoclinic structure with a space group of $C2/c$ (no. 15) could be fitted most satisfactorily to the XRD pattern of the $NaEu(MoO_4)_2$ phosphor. The weighted profile R-factors; R_{wp}, R_e, S and R_F are 1.690%, 0.737%, 2.2936 and 2.816%, respectively, and these values provide information on the phase purity of the sample prepared in this study. The representative XRD pattern of the $NaEu(MoO_4)_2$ phosphor prepared using the WASSR method is shown in Fig. 2. The detailed crystallographic data and structure refinement parameters obtained by Rietveld refinement analysis are summarised in Tables 1 and 2. The lattice parameters of the $NaEu(MoO_4)_2$ sample prepared by the WASSR method were found to be $a = 0.74214(6)$, $b = 1.14644(1)$, $c = 0.52475(4)$ nm, $\beta = 134.999(4)°$ and $V = 0.31570(4)$ nm^3, respectively. The refined cell parameters of the sample synthesized by the SSR method are also listed in Table 1. The refined structural parameters are given in Fig. S1 and Table S2 in ESI.† The values of the lattice parameters of $NaEu(MoO_4)_2$ prepared by the WASSR method matched well with those of $NaEu(MoO_4)_2$ prepared by the conventional SSR method. The site occupancies

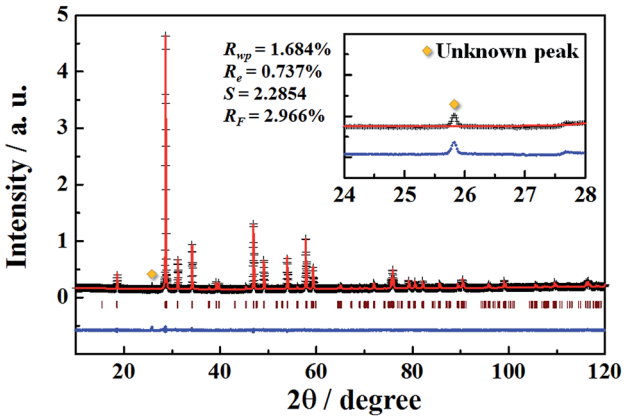

Fig. 2 Observed (+) and calculated (red line) XRD pattern of $NaEu(MoO_4)_2$ nano-phosphor prepared by WASSR method as well as the difference profile (blue bottom line) of the two patterns. Bragg reflection peak positions are shown as vertical bars. Inset shows the enlarged diffraction patterns in the range of 24–28°.

Table 1 Crystallographic parameters for $NaEu(MoO_4)_2$ prepared by the WASSR method and the conventional SSR method

$NaEu(MoO_4)_2$		
	WASSR method	SSR method
Crystal system	Monoclinic	Monoclinic
Space group	*C*2/*c*	*C*2/*c*
a (nm)	0.74214(6)	0.74188(5)
b (nm)	1.14644(1)	1.14716(1)
c (nm)	0.52475(4)	0.52452(5)
β (°)	134.999(4)	134.994(4)
V (nm^3)	0.31570(4)	0.31568(4)

Table 2 Refined structural parameters of the $NaEu(MoO_4)_2$ phosphor obtained by Rietveld refinement using the XRD data recorded at room temperature[a]

$NaEu(MoO_4)_2$						
Atom	Site	Occupancy	*x*	*y*	*z*	U_{iso} (nm^2)
Eu1	4e	0.504(3)	0	0.1210(4)	1/4	0.0094(5)
Na1	4e	0.4961	0	0.12096	1/4	0.00943
Mo1	4e	1	0	0.6266(3)	1/4	0.0076(4)
O1	8f	1	0.127(1)	0.2950(6)	0.077(2)	0.013(1)
O2	8f	1	0.224(2)	0.0381(5)	0.143(2)	0.01271

[a] Because of the disordering of Eu and Na atoms, the fractional coordinate and atomic displacement parameters (U_{iso}) were constraint to the same values, respectively.

of Na1 and Eu1 (4e site) were found to be 0.4961 and 0.504(3), respectively, indicating a Na/Eu ratio of 1 : 1 in the crystal lattice. Therefore, the chemical composition of the obtained $NaEu(MoO_4)_2$ sample was found to be stoichiometric. Fig. 3 shows the crystal structure of $NaEu(MoO_4)_2$ illustrated using the VESTA program based on the crystallographic data obtained by Rietveld refinement analysis.[22] Na^+ and Eu^{3+} ions occupy the

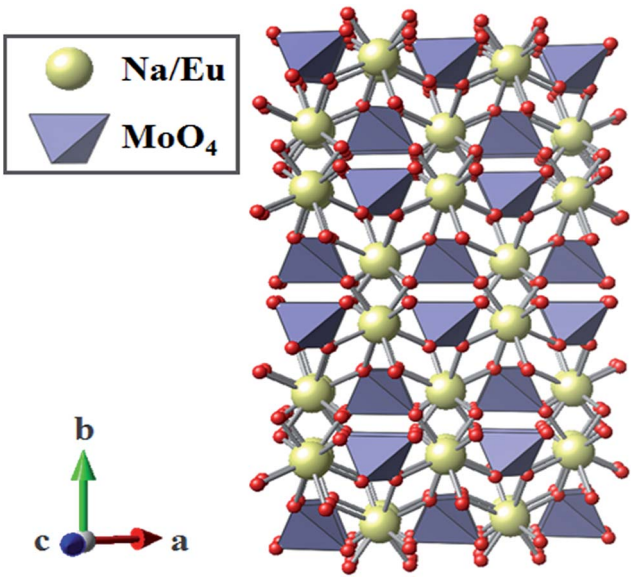

Fig. 3 Crystal structure obtained by Rietveld analysis for the $NaEu(MoO_4)_2$ nano-phosphor synthesized by the WASSR method.

same dodecahedral sites and the site occupancy of Na^+/Eu^{3+} is 1 : 1. Mo^{6+} ions are coordinated with four oxide anions to form a tetrahedron and do not share any edges or corners themselves. The bonding distances between the cation and anion in the $NaEu(MoO_4)_2$ phosphors synthesized by WASSR and conventional SSR methods are listed in Table S3 in the ESI.†

SEM images of the $NaEu(MoO_4)_2$ phosphors prepared by the WASSR and SSR methods are depicted in Fig. 4. Both the $NaEu(MoO_4)_2$ phosphors prepared by the WASSR and SSR methods exhibit a granular particle morphology. The particle size of the sample prepared by the WASSR method is smaller than that of the sample prepared by the conventional SSR method. The average particle size of the sample prepared by the WASSR method is ~200 nm. The $NaEu(MoO_4)_2$ sample prepared by the WASSR method exhibited no signs of strong sintering of the particles, which contributes to the distribution of individual particles. On the other hand, the $NaEu(MoO_4)_2$ sample prepared by the SSR method underwent strong sintering, which could be attributed to the heat treatment employed at high temperatures.

Photoluminescence properties

Fig. 5 shows the excitation and emission spectra of the $NaEu(MoO_4)_2$ phosphor prepared by the WASSR method. The excitation spectrum exhibits a strong, broad band from 220 to 350 nm, corresponding to the charge transfer (CT) transition between O^{2-} and Eu^{3+}. A few strong narrow peaks observed in the range of 350–500 nm could be attributed to the 4f–4f transitions of Eu^{3+}.[23] All emission peaks of the $NaEu(MoO_4)_2$ phosphor correspond to the transition occurring from $^5D_0$ excited level to the ^7F_J (J = 0, 1, 2, 3 and 4) ground levels of Eu^{3+}. Generally, the $^5D_0 \rightarrow {}^7F_2$ electric dipole transition, which is induced by the lack of inversion symmetry at the Eu^{3+} site, is more sensitive to the site symmetry than the $^5D_0 \rightarrow {}^7F_1$

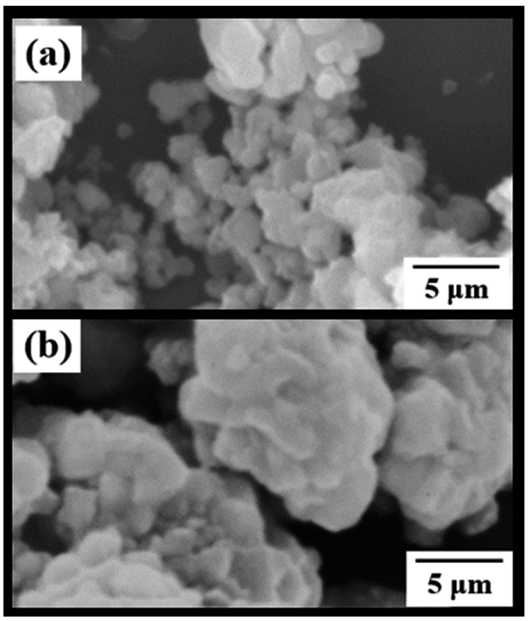

Fig. 4 SEM images of $NaEu(MoO_4)_2$ phosphors synthesized with the (a) WASSR method and (b) conventional SSR method.

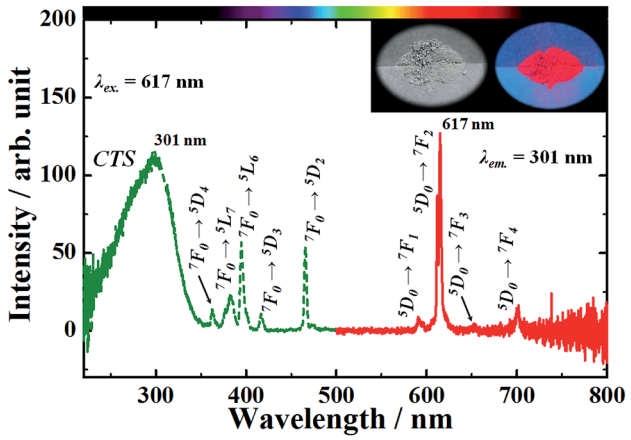

Fig. 5 Excitation and emission spectra of the $NaEu(MoO_4)_2$ phosphor. Inset shows the photographs of the phosphor material under (left) a fluorescent lamp and (right) UV light of 365 nm.

magnetic dipole transition. When an Eu^{3+} ion is located at the low inversion symmetry site, the emission intensity of the $^5D_0 \rightarrow {}^7F_2$ electric dipole transition is relatively higher than that of the $^5D_0 \rightarrow {}^7F_1$ magnetic dipole transition.[23] In the emission spectrum, the peak intensity corresponding to $^5D_0 \rightarrow {}^7F_2$ electric dipole transition at 617 nm is more dominant than that of the $^5D_0 \rightarrow {}^7F_1$ and $^7F_3$ magnetic dipole transitions observed at 595 nm and 650 nm. This indicates that the EuO_8 dodecahedron in the crystal lattice has a low inversion symmetry and that the $NaEu(MoO_4)_2$ phosphor is suitable for use as red-emitting phosphors because the ideal emission for a rich red colour corresponds to a narrow band observed ~610 nm.[23]

Effect of Gd^{3+} doping on the photoluminescence properties

When luminescence ions beyond a critical concentration are doped into host materials, the emission intensity of the phosphor reduces due to concentration quenching. The $NaEu(MoO_4)_2$ phosphor contains a large amount of Eu^{3+} ions in the crystal lattice as compared to the previously reported Eu^{3+}-doped phosphors.[24–29] Therefore, it is necessary to reduce the Eu^{3+} content in the crystal lattice to effectively enhance the emission intensity of the $NaEu(MoO_4)_2$ phosphor. In this study, Gd^{3+} (ionic radius: 0.1053 nm for 8 coordination[30]) was doped into the Eu^{3+} (ionic radius: 0.1066 nm for 8 coordination[30]) site to enhance the emission intensity of the $NaEu(MoO_4)_2$ phosphor. Gd^{3+} has an identical valence and similar ionic radius as those of Eu^{3+} and does not exhibit any optical absorption or emission bands in the visible light region. Therefore, Gd^{3+} doping would be the most promising strategy to reduce the Eu^{3+} content in the crystal lattice without significantly changing the crystallographic environment around Eu^{3+}. Fig. 6 shows the XRD patterns of the $NaEu_{1-x}Gd_x(MoO_4)_2$ ($0 \leq x \leq 0.50$) phosphors prepared by the WASSR method. Although weak secondary unknown peaks appeared in the XRD patterns of all samples, almost all of the XRD peaks were well indexed to the single-phase monoclinic $NaEu(MoO_4)_2$. However, in addition, the peak intensity of MoO_3 did not change with an increase in the Gd^{3+} content in the $NaEu_{1-x}Gd_x(MoO_4)_2$ ($0 \leq x \leq 0.50$) phosphors. The XRD peaks corresponding to monoclinic $NaEu(MoO_4)_2$ shifted to a higher diffraction angle with an increase in the Gd^{3+} content in the $NaEu_{1-x}Gd_x(MoO_4)_2$ ($0 \leq x \leq 0.50$) phosphors. Additionally, the refined lattice volume of the $NaEu_{0.70}Gd_{0.30}(MoO_4)_2$ phosphor was found to be 0.3150(3) nm^3, as comparable to that of the Gd^{3+} non-doped $NaEu(MoO_4)_2$ phosphor ($V = 0.31571(4)$ nm^3). The refinement data are summarised in Table S7 in ESI.† These results indicate that $NaEu(MoO_4)_2$ was formed as the main phase in all the samples and small Gd^{3+} ions were successfully substituted into the Eu^{3+} site in the crystal lattice.

Fig. 7(a) shows the excitation and emission spectra of $NaEu_{1-x}Gd_x(MoO_4)_2$ ($x = 0$ and 0.30) phosphors. The emission

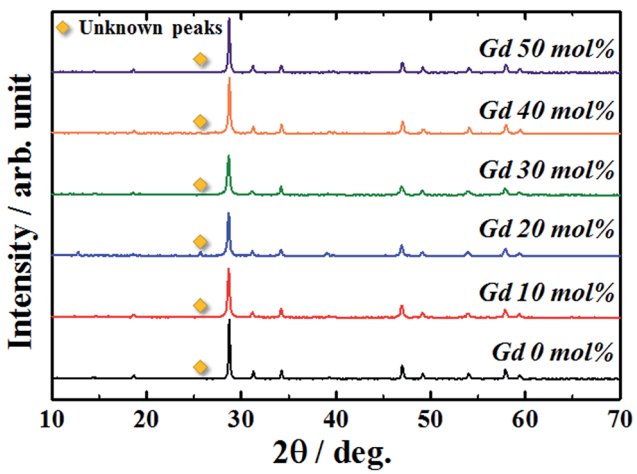

Fig. 6 Crystal structure obtained by Rietveld analysis for the $NaEu(MoO_4)_2$ nano-phosphor synthesized by the WASSR method.

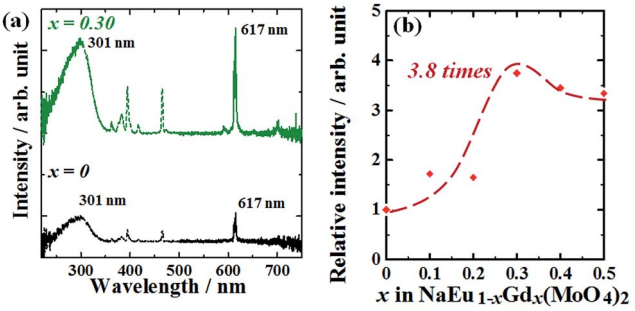

Fig. 7 (a) Excitation and emission spectra of $NaEu_{1-x}Gd_x(MoO_4)_2$ (x = 0 and 0.30) phosphors. (b) Dependence of the emission intensity on the Gd^{3+} concentration in the $Na(Eu_{1-x}Gd_x)(MoO_4)_2$ ($0 \le x \le 0.50$) nano-phosphors.

profiles of all samples were essentially the same without exhibiting a change in the ratio of peak intensity corresponding to the $^5D_0 \rightarrow {}^7F_2$ and $^5D_0 \rightarrow {}^7F_1$ transitions on introducing Gd^{3+} ions into the $NaEu(MoO_4)_2$ phosphor. This indicates that the inversion symmetry of the EuO_8 dodecahedron in the $NaEu(MoO_4)_2$ crystal lattice was well maintained even on doping a large amount of Gd^{3+} ions in the crystal lattice. However, a clear difference is recognised in the emission intensity of these spectra. The emission intensity increased with an increase in the Gd^{3+} content and reached a maximum value at $x = 0.30$ in the $NaEu_{1-x}Gd_x(MoO_4)_2$ ($0 \le x \le 0.50$) phosphors. The emission intensity of the $NaEu_{0.70}Gd_{0.30}(MoO_4)_2$ phosphor was ~3.8 times higher than that of the $NaEu(MoO_4)_2$ phosphor, and the relative emission intensity of this phosphor was 17% of the value obtained with the commercial $Y_2O_3 : Eu^{3+}$ phosphor.

Conclusions

The red-emission $NaEu_{1-x}Gd_x(MoO_4)_2$ ($0 \le x \le 0.50$) phosphors were synthesized using the WASSR method, and their crystal structure and photoluminescence properties were investigated. $NaEu(MoO_4)_2$ exhibits a monoclinic structure with a space group $C2/c$ (no. 15), which is composed of a Na/EuO_8 dodecahedron and MoO_4 tetrahedron. The $NaEu(MoO_4)_2$ structure was found to be the main phase in all the $NaEu_{1-x}Gd_x(MoO_4)_2$ ($0 \le x \le 0.50$) phosphors. These phosphors exhibited a strong, narrow red emission owing to the energy transfer occurring from $^5D_0$ excited level to the ^7F_J ($J = 0, 1, 2, 3$, and 4) ground levels of Eu^{3+}, and the emission intensity of the phosphors was successfully enhanced by doping the $NaEu(MoO_4)_2$ phosphor with Gd^{3+} ions. The optimization of the Gd^{3+} content resulted in the highest emission intensity for the sample $NaEu_{0.70}Gd_{0.30}(MoO_4)_2$, with the emission intensity of the phosphor being ~3.8 times higher than that of the $NaEu(MoO_4)_2$ ($x = 0$) phosphor. The average particle size of the $NaEu_{1-x}Gd_x(MoO_4)_2$ ($0 \le x \le 0.50$) phosphors obtained by the WASSR method was ~200 nm.

Notes and references

1 A. F. Khan, D. Haranath, R. Yadav, S. Singh, S. Chawla and V. Dutta, *Appl. Phys. Lett.*, 2008, **93**, 073103.
2 X. Li, Q. Li, J. Wang, S. Yang and H. Liu, *Opt. Mater.*, 2007, **29**, 528.
3 G. Yi, H. Lu, S. Zhao, Y. Ge, W. Yang, D. Chen and L. H. Guo, *Nano Lett.*, 2004, **4**, 2191.
4 D. Haranath, H. Chander, P. Sharma and S. Singh, *Appl. Phys. Lett.*, 2006, **89**, 173118.
5 H. Yang, D. K. Lee and Y. S. Kim, *Mater. Chem. Phys.*, 2009, **114**, 665.
6 A. Shalav, B. S. Richards, T. Trupke, K. W. Krämer and H. U. Güdel, *Appl. Phys. Lett.*, 2005, **86**, 013505.
7 M. Kakihana, *J. Sol-Gel Sci. Technol.*, 1996, **6**, 7.
8 K. J. Laidler, *J. Chem. Educ.*, 1984, **61**, 494.
9 J. Wang, Y. Xua, M. Hojamberdiev, Y. Cui, H. Liu and G. Zhu, *J. Alloys Compd.*, 2009, **479**, 772.
10 C. A. Kodaira, H. F. Brito, O. L. Malta and O. A. Serra, *J. Lumin.*, 2003, **101**, 11.
11 S. W. Kim, T. Kaneko, K. Toda, K. Uematsu, T. Ishigaki, M. Sato, J. Koide, M. Toda and Y. Kudo, in *Proceeding of IDW'15*, 2014, vol. 21, p. 510.
12 T. Kaneko, S. W. Kim, A. Toda, K. Uematsu, T. Ishigaki, K. Toda, M. Sato, J. Koide, M. Toda, Y. Kudo, T. Masaki and D. H. Yoon, *Sci. Adv. Mater.*, 2015, **7**, 1502.
13 K. Toda, S. W. Kim, T. Hasegawa, M. Watanabe, T. Kaneko, A. Toda, A. Itadani, M. Sato, K. Uematsu, T. Ishigaki, J. Koide, M. Toda, Y. Kudo, T. Masaki and D. H. Yoon, *Key Eng. Mater.*, 2016, **690**, 268.
14 S. W. Kim, T. Hasegawa, M. Watanabe, K. Sugimoto, Y. Saito, K. Uematsu, K. Toda and M. Sato, *Dyes Pigm.*, 2017, **136**, 219.
15 S. W. Kim, K. Toda, T. Hasegawa, M. Watanabe, T. Kaneko, A. Toda, A. Itadani, M. Sato, K. Uematsu, T. Ishigaki, J. Koide, M. Toda, Y. Kudo, T. Masaki and D. H. Yoon, *Sci. Adv. Mater.*, 2016, accepted.
16 Z. Wang, H. Liang, M. Gong and Q. Su, *Mater. Lett.*, 2008, **62**, 619.
17 Y. Zhang, S. Shi, J. Gao and J. Zhou, *J. Nanosci. Nanotechnol.*, 2010, **10**, 2156.
18 Z. Wang, H. Liang, L. Zhou, J. Wang, M. Gong and Q. Su, *J. Lumin.*, 2008, **128**, 147.
19 Z. Wang, H. Liang, M. Gong and Q. Su, *Opt. Mater.*, 2007, **29**, 896.
20 F. Izumi and K. Momma, *Solid State Phenom.*, 2007, **130**, 15.
21 A. Arakcheeva, D. Logvinovich, G. Chapuis, V. Morozov, S. V. Eliseeva, J. C. G. Bünzli and P. Pattison, *Chem. Sci.*, 2012, **3**, 384.
22 K. Momma and F. Izumi, *J. Appl. Crystallogr.*, 2011, **44**, 1272.
23 T. Kano, in *Phosphor Handbook*, ed. W. M. Yen, S. Shionoya and H. Yamamoto, CRC Press, Boca Raton, FL, 2nd edn, 2006, pp. 191–214.
24 J. Dhanaraj, R. Jagannathan, T. R. N. Kutty and D. H. Lu, *J. Phys. Chem. B*, 2001, **105**, 11098.
25 J. H. Jeong, J. S. Bae, S. S. Yi, J. C. Park and Y. S. Kim, *J. Phys.: Condens. Matter*, 2003, **15**, 567.
26 S. W. Kim, T. Masui and N. Imanaka, *Electrochemistry*, 2009, **77**, 611.

27 Y. S. Chang, F. M. Huang, Y. Y. Tsai and L. G. Teoh, *J. Lumin.*, 2009, **129**, 1181.
28 S. M. Kim, T. Masui and N. Imanaka, *ECS J. Solid State Sci. Technol.*, 2012, **1**, R41.
29 V. Dubey, J. Kaur, S. Agrawal, N. S. Suryanarayana and K. V. R. Murthy, *Optik*, 2013, **124**, 5585.
30 R. D. Shannon, *Acta Crystallogr., Sect. A: Cryst. Phys., Diffr., Theor. Gen. Crystallogr.*, 1976, **32**, 751.